Cell Medicine, Vol. 9, pp. 73–85, 2017
Printed in the USA.

2155-1790/17 $90.00 + .00
DOI: https://doi.org/10.3727/215517916X693384
www.cognizantcommunication.com

Neurovascular Cell Sheet Transplantation in a Canine Model of Intracranial Hemorrhage

Woo-Jin Lee,*†[1] Jong Young Lee,‡[1] Keun-Hwa Jung,*† Soon-Tae Lee,*† Hyo Yeol Kim,§ Dong-Kyu Park,† Jung-Suk Yu,† So-Yun Kim,† Daejong Jeon,† Manho Kim,†‡ Sang Kun Lee,*† Jae-Kyu Roh,*†¶ and Kon Chu*†

*Department of Neurology, Seoul National University Hospital, College of Medicine, Seoul National University, Seoul, South Korea
†Laboratory for Neurotherapeutics, Biomedical Research Institute, Seoul National University Hospital, Seoul, South Korea
‡Department of Neurosurgery, Kangdong Sacred Heart Hospital, Seoul, South Korea
§Department of Otorhinolaryngology-Head and Neck Surgery, Samsung Medical Center, Sungkyunkwan University School of Medicine, Seoul, South Korea
¶Department of Neurology, The Armed Forces Capital Hospital, Gyeunggido, South Korea

Cell-based therapy for intracerebral hemorrhage (ICH) has a great therapeutic potential. However, methods to effectively induce direct regeneration of the damaged neural tissue after cell transplantation have not been established, which, if done, would improve the efficacy of cell-based therapy. In this study, we aimed to develop a cell sheet with neurovasculogenic potential and evaluate its usefulness in a canine ICH model. We designed a composite cell sheet made of neural progenitors derived from human olfactory neuroepithelium and vascular progenitors from human adipose tissue-derived stromal cells. We also generated a physiologic canine ICH model by manually injecting and then infusing autologous blood under arterial pressure. We transplanted the sheet cells (cell sheet group) or saline (control group) at the cortex over the hematoma at subacute stages (2 weeks from ICH induction). At 4 weeks from the cell transplantation, cell survival, migration, and differentiation were evaluated. Hemispheric atrophy and neurobehavioral recovery were also compared between the groups. As a result, the cell sheet was rich in extracellular matrices and expressed neurotrophic factors as well as the markers for neuronal development. After transplantation, the cells successfully survived for 4 weeks, and a large portion of those migrated to the perihematomal site and differentiated into neurons and pericytes (20% and 30% of migrated stem cells, respectively). Transplantation of cell sheets alleviated hemorrhage-related hemispheric atrophy ($p=0.042$) and showed tendency for improving functional recovery ($p=0.062$). Therefore, we concluded that the cell sheet transplantation technique might induce direct regeneration of neural tissue and might improve outcomes of intracerebral hemorrhage.

Key words: Cell sheet; Cell therapy; Intracerebral hemorrhage (ICH); Neurovascular progenitor; Transplantation

INTRODUCTION

Stroke is a great threat to human health, with high mortality and morbidity rates[1]. Intracerebral hemorrhage (ICH) accounts for 10%–20% of all strokes; it has a higher mortality rate (approximately 40%) and results in more severe sequelae compared to the other subtypes of stroke[1]. ICH treatment aims to minimize the expansion of the hematoma or alleviate the increased intracranial pressure in the acute stage. However, the outcomes of ICH have not significantly improved over the decades[2], although early surgical treatments including decompressive craniectomy or hematoma evacuation have been recognized to be beneficial in selected situations[3–5]. Hence, cell therapy has been actively evaluated to regenerate the damaged neurons and ultimately improve the long-term outcomes[6–11]. However, the major mechanisms of their efficacy are

Received September 27, 2016; final acceptance December 15, 2016. Online prepub date: December 21, 2016.
[1]These authors provided equal contribution to this work.
Address correspondence to Keun-Hwa Jung, M.D., Ph.D., Department of Neurology, Seoul National University Hospital, 101 Daehak-ro, Jongno-gu, Seoul 110-744, South Korea. Tel: +82-2-20724901; Fax: +82-2-36724949; E-mail: jungkh@gmail.com *or* Kon Chu, M.D., Ph.D., Department of Neurology, Seoul National University Hospital, 101 Daehak-ro, Jongno-gu, Seoul 110-744, South Korea. Tel: +82-2-2072-1878; Fax: + 82-2-2072-7424; E-mail: stemcell.snu@gmail.com

limited to the amelioration of the inflammatory response and the modulation of the damaged site to a cytoprotective microenvironment, known as the bystander effect, rather than the direct migration of the stem cells and true regeneration of the damaged tissue[7,8,11–14].

Therefore, further efforts have been designed to effectively deliver stem cells to the relevant sites, improve the viability of the transplanted stem cells, and induce direct tissue regeneration from stem cells, including scaffold-based cells, microtissue, and cell sheet technology[12,15–17]. A cell sheet, a confluent monolayer of cells grown in a cell culture dish, is a novel scaffold-free cell delivery system that can be easily manipulated considering the purpose of use, directly transplanted to the target site, and react in response to changes in their environment without causing any immunologic reaction[16]. Cell sheets have been successfully applied to a variety of tissues including the skin, cornea, myocardium, blood vessels, and muscle[12,15,18–27].

A cell sheet study ideally requires a large animal model, but for ICH it has been limited owing to the lack of relevant large-animal models. Relatively recently, a canine physiologic model of ICH was established[6], which has the following potent advantages over the previously used murine ICH model. First, compared to the murine ICH model with an intracerebral injection of collagenase[7,9,11], the canine model induces ICH via the infusion of autologous blood under arterial pressure and is therefore more physiologic. Second, with the autologous blood infusion method, the volume of ICH and the disease severity can be easily homogenized among the animals. Third, the canine brain is bigger than the murine brain; therefore, it is more suitable for the transplantation of cell sheets that have approximately 6 cm^2 of surface area[22]. Fourth, with the canine model, a more detailed neurobehavioral test can be performed to access the comprehensive functional outcomes.

In the current study, we designed a composite cell sheet made of neural progenitors, derived from human olfactory neuroepithelial cells (ONECs), and vascular progenitors, from human adipose tissue-derived stromal cells (ATSCs), to generate new neurovascular cells with trophic and regenerative support. We transplanted the composite cell sheet in the subacute stage in a canine model of ICH and evaluated its efficacy for direct neural regeneration at the relevant site and improving the histologic and clinical outcomes of ICH.

MATERIALS AND METHODS

Ethical Approval

All procedures were approved by the Institutional Animal Care and Use Committee (IACUC) of the Seoul National University Hospital. Informed consent was obtained from all individual participants included in the study. For collection and use of human cells, all procedures were approved by the institutional review boards of the Seoul National University Hospital and the Samsung Medical Center in compliance with the principles of Good Clinical Practice and the Declaration of Helsinki.

Cell Sheet Generation

We prepared human ONECs and human ATSCs for generating a cell sheet with neurovascular characteristics using previously described methods[7,28,29]. ONECs were derived from the pooled olfactory neuroepithelium of two individuals (males aged 23 and 27 years), as previously described, with a slight modification[28,29]. In brief, after local anesthetic application at the middle turbinate or the septum in the dorsomedial area, 2-mm^2 olfactory mucosal epithelium biopsy was performed by an ear, nose, and throat surgeon using a rigid endoscope. The harvested olfactory tissue specimen was immersed in Dulbecco's modified Eagle's medium (DMEM)/HAM F12 culture medium (Invitrogen, Carlsbad, CA, USA) and dissected into several pieces ranging in thickness from 200 to 500 μm. Then 500 μl of culture medium containing DMEM/HAM F12 with 10% fetal calf serum (Invitrogen) and 1% penicillin/streptomycin (Invitrogen) was added to each culture dish and replaced every 2 days. For ATSCs, we acquired stromal vascular fractions from the pooled human subcutaneous adipose tissue of three individuals (one male and two females, aged 22 to 30 years) by digestion with 0.075% collagenase type I (Invitrogen), as previously described[7,30]. In brief, after removing the mature adipocyte fraction from the stromal vascular fractions by centrifuging at 1,200×*g* for 10 min, the remaining fractions were treated with red blood cell lysis buffer (Sigma-Aldrich, St. Louis, MO, USA) and then filtered through a 100-μm nylon mesh (Anping County Bolin Metal Wire Mesh, Hengshui, P.R. China) to remove the erythrocyte debris. The obtained cells were incubated with endothelial growth medium (EGM-2; Clonetics, Walkersville, MD, USA) for 1 h and then maintained in DMEM/HAM F12 along with 10% fetal calf serum (Invitrogen), 1% penicillin/streptomycin (Invitrogen), and N2 supplement (Gibco Life Technologies, Rockville, MD, USA). To generate a cell sheet composed of ATSCs and ONECs, cells were seeded on double-coated six-well plates [poly-L-lysine (PLL) and laminin; Sigma-Aldrich] in high-glucose DMEM, 15% fetal bovine serum (FBS; Gibco), 1% non-essential amino acids (NEAA; Gibco), 1% L-glutamine (Gibco), and 0.05 mM β-mercaptoethanol (Gibco), with 10^3 U/ml of human leukemia inhibitory factor (LIF; Chemicon, Temecula, CA, USA) and penicillin/streptomycin (Gibco). Cells were maintained by partial media replacement every 3 days, without splitting, in order to allow

mixed cells to become confluent. After approximately 4 weeks, the cells formed a sheet of progenitor cells interconnected with a layer of stromal cells.

In Vitro Analysis of the Cell Sheet

The cell sheet was gently peeled off the PLL- and laminin-coated plate. To examine the multipotent characteristics, we conducted reverse transcription polymerase chain reaction (RT-PCR) for V-Myc avian myelocytomatosis viral oncogene homolog (*c-MYC*), Musashi RNA-binding protein 1 (*MSI1*), *MSI2*, sex-determining region Y box 2 (*SOX2*), nestin, vascular endothelial growth factor (*VEGF*), nerve growth factor (*NGF*), brain-derived neurotrophic factor (*BDNF*), epidermal growth factor (*EGF*), IGF-1 receptor (*IGF1R*), *EGFR*, Fms-related tyrosine kinase 1 (*FLT1* or *VEGFR1*), microtubule-associated protein 2 (*MAP2*), and glial fibrillary-associated protein (*GFAP*), as previously described[11,31]. Total RNA was isolated from the homogenates of the sheet using TRI reagent (Sigma-Aldrich), and semiquantitative RT-PCR was performed with the primer sets described in Table 1. For scanning electron microscopy (SEM; Carl Zeiss, Germany), transmission electron microscopy (TEM; FEI, Hillsboro, OR, USA), and immunocytochemistry, cell sheets were grown on coverslips and were fixed with 3% glutaraldehyde (Sigma-Aldrich) in 0.1 M Na cacodylate-buffered solution (Sigma-Aldrich). For SEM, the cell sheet was fixed in 1% osmium tetroxide (Sigma-Aldrich), dehydrated in acetone (Sigma-Aldrich), dried with CO_2, and coated with a layer of gold (Gibco). For TEM, the cell sheets were detached from the coverslip in Epon (Gibco) after being processed using the procedure used in SEM. Sections (60 to 100 nm thick) were stained with lead citrate (Sigma-Aldrich) and uranium acetate (Sigma-Aldrich). To perform immunocytochemistry analysis, the cell sheet was immunostained with antibodies against collagen III, fibronectin, nestin, vimentin, oligodendrocyte 4 (O4), smooth muscle actin (SMA), laminin, and Ki-67

Table 1. Primer Sequences for the Semiquantitative RT-PCR Analysis

Gene	Primer Sequences	Size (bp)	Annealing (°C)	GenBank Accession
Self-renewal, proliferation				
myc	Forward: 5′-GGCTCCTGGCAAAAGGTCA-3′	119	62.2	NM_002467
	Reverse: 5′-CTGCGTAGTTGTGCTGATGT-3′			
Msi1	Forward: 5′-CTGTCGGTGAACACCACGG-3′	125	62.9	NM_002442
	Reverse: 5′-AACGTGACAAACCCGAACCC-3′			
Msi2	Forward: 5′-ATCCCACTACGAAACGCTCC-3′	116	61.7	NM_138962
	Reverse: 5′-GGGGTCAATCGTCTTGGAATC-3′			
Neuronal differentiation				
sox2	Forward: 5′-TACAGCATGTCCTACTCGCAG-3′	110	61.4	NM_003106
	Reverse: 5′-GAGGAAGAGGTAACCACAGGG-3′			
nestin	Forward: 5′-CAACAGCGACGGAGGTCTC-3′	164	62.4	NM_006617
	Reverse: 5′-GCCTCTACGCTCTCTTCTTTGA-3′			
MAP2	Forward: 5′-TGGTGCCGAGTGAGAAGAAG-3′	91	61.5	NM_001039538
	Reverse: 5′-AGTGGTTGGTTAATAAGCCGAAG-3′			
NGF	Forward: 5′-GGCAGACCCGCAACATTACT-3′	135	62.5	NM_002506
	Reverse: 5′-CACCACCGACCTCGAAGTC-3′			
BDNF	Forward: 5′-GGCTTGACATCATTGGCTGAC-3′	79	61.6	NM_001143811
	Reverse: 5′-CATTGGGCCGAACTTTCTGGT-3′			
GFAP	Forward: 5′-CTGCGGCTCGATCAACTCA-3′	209	62.1	NM_001242376
	Reverse: 5′-TCCAGCGACTCAATCTTCCTC-3′			
Cell proliferation, cellular integrity				
EGF	Forward: 5′-TGGATGTGCTTGATAAGCGG-3′	223	60.2	NM_001178131
	Reverse: 5′-ACCATGTCCTTTCCAGTGTGT-3′			
EGFR	Forward: 5′-AGGCACGAGTAACAAGCTCAC-3′	177	62.3	NM_201284
	Reverse: 5′-ATGAGGACATAACCAGCCACC-3′			
flt1	Forward: 5′-TTTGCCTGAAATGGTGAGTAAGG-3′	117	60.7	NM_001159920
	Reverse: 5′-TGGTTTGCTTGAGCTGTGTTC-3′			
VEGF	Forward: 5′-GAGGAGCAGTTACGGTCTGTG-3′	96	62.1	NM_005429
	Reverse: 5′-TCCTTTCCTTAGCTGACACTTGT-3′			
IGF1R	Forward: 5′-AGGATATTGGGCTTTACAACCTG-3′	80	60.0	NM_000875
	Reverse: 5′-GAGGTAACAGAGGTCAGCATTTT-3′			

(1:100; all from Chemicon), as previously described[7,31]. They were counterstained with 1 μg/ml 4′,6-diamidino-2-phenylindole (DAPI; Sigma-Aldrich). Images were captured and assessed using a digital camera and software (LSM 510; Carl Zeiss Microimaging, Thornwood, NY, USA).

Animals

Twenty-four mature (age: 24–36 months), morphologically normal, male mongrel dogs with a similar weight (20–26 kg) were studied. Each animal was designated an admission number by the Animal Care and Use Committee of Seoul National University Hospital. All animals were managed with standardized procedures approved by the IACUC of Seoul National University Hospital. Twelve dogs were assigned to undergo saline treatment (the control group), and 12 dogs received cell sheet transplantation after ICH induction (the cell sheet group). All dogs underwent physiological monitoring, imaging, a neurologic test, and histological examination.

Experimental ICH Induction

The surgical procedure for ICH induction was performed as previously described[6,32]. After an acclimatization period of 4 weeks, the animals were subjected to the ICH induction procedure. All the dogs were made to fast the night before the surgery. Anesthesia was primarily induced with intramuscular zoletil (15 mg/kg zolazepam and tiletamine; Virbac AH, Fort Worth, TX, USA) and then maintained by inhaled anesthesia with enflurane (Arylane; Ilsung Pharmaceuticals, Seoul, South Korea). The animals were mechanically ventilated using an inhalation anesthesia kit (GE Healthcare, Chalfont St. Giles, UK) during the procedure. The tidal volume and ventilatory frequency were modified to maintain a constant arterial carbon dioxide pressure (35–45 mmHg). Changes in blood pressure, heart rate, oxygen saturation, and electrocardiography parameters were also monitored throughout the procedure. A burr hole was made 4 cm posterior to the bregma and 2 cm left to the parietal eminence in a lateral to midline direction[6,32].

We required a canine ICH model to determine the long-term neurologic deficits with an acceptable mortality. However, pilot experiments with various techniques showed extreme phenotypes, from no overt neurologic deficits to early death associated with increased intracranial pressure. Eventually, we modified a previously reported technique into a stepwise technique for ICH induction[6,32], where a small amount of autologous blood (2 ml) was manually injected against the intracranial pressure via the burr hole, and subsequently 10 ml autologous blood was infused under arterial pressure through a tube with the proximal end connected to a femoral artery catheter. The distal end was connected to a spinal needle that was positioned 1 cm below the brain surface via a burr hole. The spinal needle used for introduction of the blood was kept in its position for an additional 10 min after completing infusion of blood to avoid creating an outflow tract (Fig. 1A–E).

Cell Sheet Transplantation

Two weeks after ICH induction, animals were subjected to saline or cell sheet transplantation procedures. For the cell tracking study, the cells during the sheet generation period were transfected with lentiviral green fluorescent protein (GFP) using a lentivirus marker supernatant, Lenti-Green (Biogenova, Rockville, MD, USA), which contains approximately 10^7 viral particles/ml, with a 1:1 ratio of viral supernatant volume to the volume of medium, according to the manufacturer's protocol for 2 days. On the day of transplantation, sheets were peeled off the laminin-coated plate, transferred to 200 ml of media using a pipette tip, and folded as multilayers to facilitate transplantation via a burr hole (Fig. 1G)[15,16,19,20]. After opening the dura through the burr hole made at the previous surgery, the cell sheet was gently transferred onto the brain surface and spread by adding saline drops.

Brain Magnetic Resonance Imaging

The hematoma volume and tissue atrophy were examined at 1 day and 6 weeks after ICH induction, respectively. Anesthesia for immobility during magnetic resonance imaging (MRI) was applied with an intramuscular injection of zoletil (zolazepam and tiletamine; 15 mg/kg; Virbac AH). Using a 3.0-T scanner (Magnetom Vision, Siemens, Erlangen, Germany), T1- and T2-weighted images, fluid-attenuated inversion recovery (FLAIR) images, and susceptibility-weighted imaging (SWI) scans were obtained in the transverse plane (5-mm thickness). An ICH area was defined on SWI scans as an area of lower signal intensity compared to a normal area[33], and hematoma volume was measured as the length of the long axis × the length of the short axis of the hematoma (at the section of the largest lesion) × (number of the involved slices/2) × 1/2[34]. The hemispheric area was measured on each slice of the FLAIR images at 6 weeks after ICH induction, and hemispheric atrophy (%) was calculated as [(contralateral hemisphere area − the lesion hemisphere area)/the contralateral hemisphere area] × 100. Data of the total hemispheric atrophy with ICH are shown as mean values of hemisphere atrophy from each slice.

Neurobehavioral Scoring

Neurobehavioral performance was assessed via continuous video monitoring. Neurobehavioral scoring was performed using a standardized rating scale established for canine experiments. The neurobehavioral scoring comprised semiquantitative evaluations for motor function, consciousness, head turning, circling, and hemianopia; the

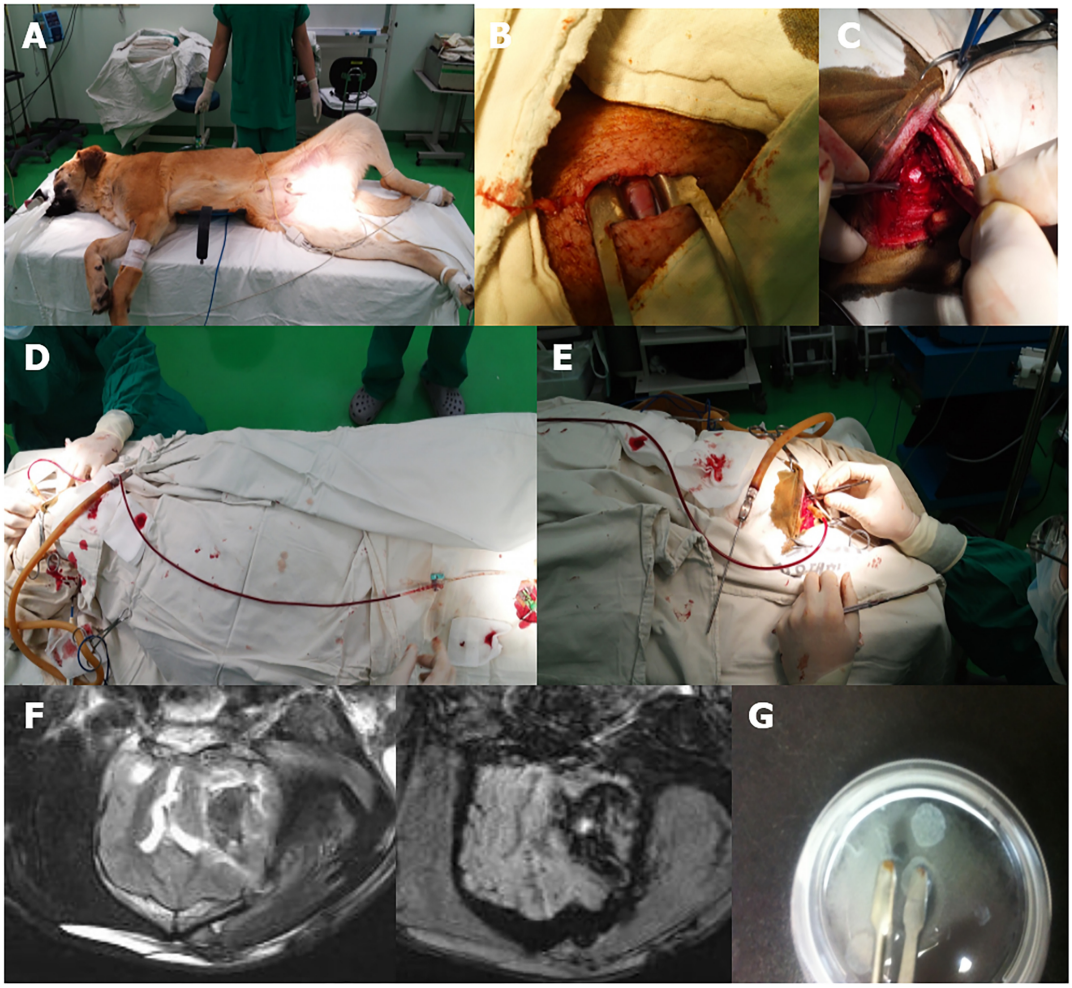

Figure 1. Intracranial hemorrhage (ICH) induction procedure. (A) Surgery position. (B) Cut-down for showing the femoral artery up. (C) Surgery for making burr hole. (D, E) Connecting a line from the femoral catheter to the spinal needle into the left cranium for conveying blood under arterial pressure. (F) Mortality case demonstrating brain herniation by the mass effect of hematoma [T2-weighted imaging (T2WI) and susceptibility-weighted imaging (SWI)]. (G) Preparation of cell sheet at the day of transplantation.

score ranged from 2 (completely normal) to 11 (comatose or dead) (Fig. 2)[35,36]. Each canine was serially assessed prior to anesthesia, daily during the first week, and then weekly until euthanasia at 6 weeks.

Immunohistochemistry of Brain Tissues

At the end of neurobehavioral testing (6 weeks after ICH or 4 weeks after cell sheet treatment), the dogs were euthanized. The brain was harvested and fixed in 4% paraformaldehyde (Sigma-Aldrich) before processing. After 24 h, the brain was divided into the two hemispheres and the brainstem; the hemisphere ipsilateral to ICH was further dissected into the perihematomal region including the blood and cell sheet injection site, and the other brain regions. After cryoprotection using 30% sucrose (Sigma-Aldrich) for 24 h, the specimens were cut into 1-cm^3 blocks and then frozen. Using a cryostat (CM 1900; Leica, Deerfield, IL, USA), each block was sectioned to obtain 40-μm slices. To examine the phenotypic differentiation of transplanted cells, sections were immunostained with an antibody against GFP and against different cell markers of neurons, pericytes, and endothelial cells. Sections were labeled with chicken anti-GFP (1:500; AB290; Abcam, Cambridge, MA), anti-nestin (1:200; Chemicon), anti-platelet-derived growth factor receptor β (PDGFRβ; 1:200; Abcam), anti-αSMA (1:100; Dako), anti-neurofilament (NF; 1:200; Chemicon), and anti-GFAP (1:200; Sigma-Aldrich) antibodies. Fluorescein isothiocyanate (FITC)-conjugated anti-sheep IgG (1:100; Biodesign, Memphis, TN, USA) and cyanine 3 (Cy3)-conjugated anti-mouse IgG antibodies (1:300; Jackson Immunoresearch Laboratories, West Grove, PA, USA) were used as secondary antibodies. Sections were counterstained with 1 μg/ml DAPI (Sigma-Aldrich). In

	Scale	Grade
Motor	1-4	No deficit=1 Hemiparetic but able to walk=2 Stands only with assistance=3 Hemiplegia and unable to stand=4
Consciousness	1-4	Normal=1 Mildly reduced=2 Severely reduced=3 Comatose=4
Head turning	0-1	Absent=0 Posturing and turns toward the side of the infarct, does not lift head, comatose, or dead=1
Circling	0-1	Absent =0 Present, does not ambulate or dead=1
Hemianopsia	0-1	Absent=0 Present=1
Total	2-11	Normal=2 Death=11

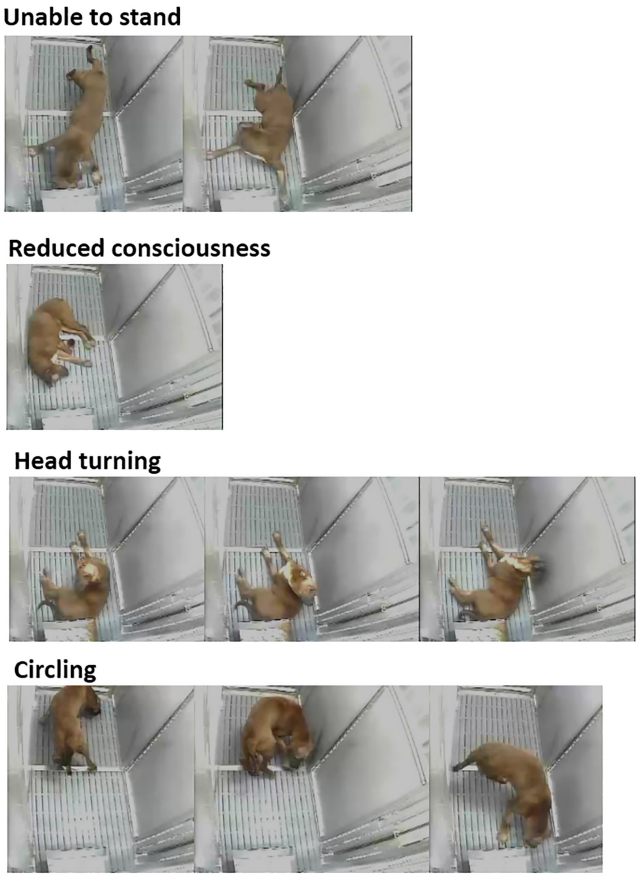

Figure 2. Scales for the neurobehavioral scoring system. A neurobehavioral test was done using a standardized rating scale via continuous video monitoring. Left: Scoring system was composed of motor function, consciousness level, head turning, circling behavior, and hemianopia, which ranged from 2 to 11. Neurological deficits relevant to some of the scoring system (motor, consciousness, head turning, and circling) were exemplified on the right side.

each section, the labeled cells were traced and analyzed using an image analysis system (LSM 510; Carl Zeiss Microimaging)[7,9,11,31].

Statistical Analysis

Data were reported as number (percentage), mean± standard deviation, or as median [interquartile range (IQR)]. For comparisons of hematoma volume, hemispheric atrophy, and neurobehavioral outcomes between the groups, data were analyzed using Mann–Whitney *U* tests. Two-tailed values of $p<0.05$ were considered significant.

RESULTS

Cell Sheet Characteristics Prior To Transplantation

The cell sheet is a layer of human ATSCs with incorporated human ONECs (Fig. 3A). On RT-PCR analysis, the cell sheet showed high expression of stem cell markers, indicating proliferation and self-renewal capacity, including *MYC*, *MSI1*, and *MSI2*. Markers specific for neuronal development, such as *SOX*2, nestin, and *MAP2*, were also markedly positive. Furthermore, the cell sheet actively expressed various cytokines known to enhance and maintain cell proliferation and survival, such as *BDNF*[37] and *VEGF*[38] (Fig. 3B). The SEM of the cell sheet sections revealed a sheet-like, organized, dense structure with high cellularity, composed of rich extracellular matrices and no necrotic core (Fig. 3C). The TEM image also demonstrated active intercellular exchange of materials (Fig. 3D). On immunohistochemistry, the cell sheet highly expressed protein markers for extracellular matrix proteins such as collagen III, fibronectin, and laminin, all of which are involved in cell differentiation, migration, and adhesion (Fig. 4A–C). Moreover, the cell sheet comprised several cell types including vimentin$^+$ stem cells (80%), nestin$^+$ neural progenitors (80%), SMA$^+$ vascular stromal cells (30%), and O4$^+$ oligodendrocytes (10%) (Fig. 4D–G). In addition, approximately 10% of the cells were positive for

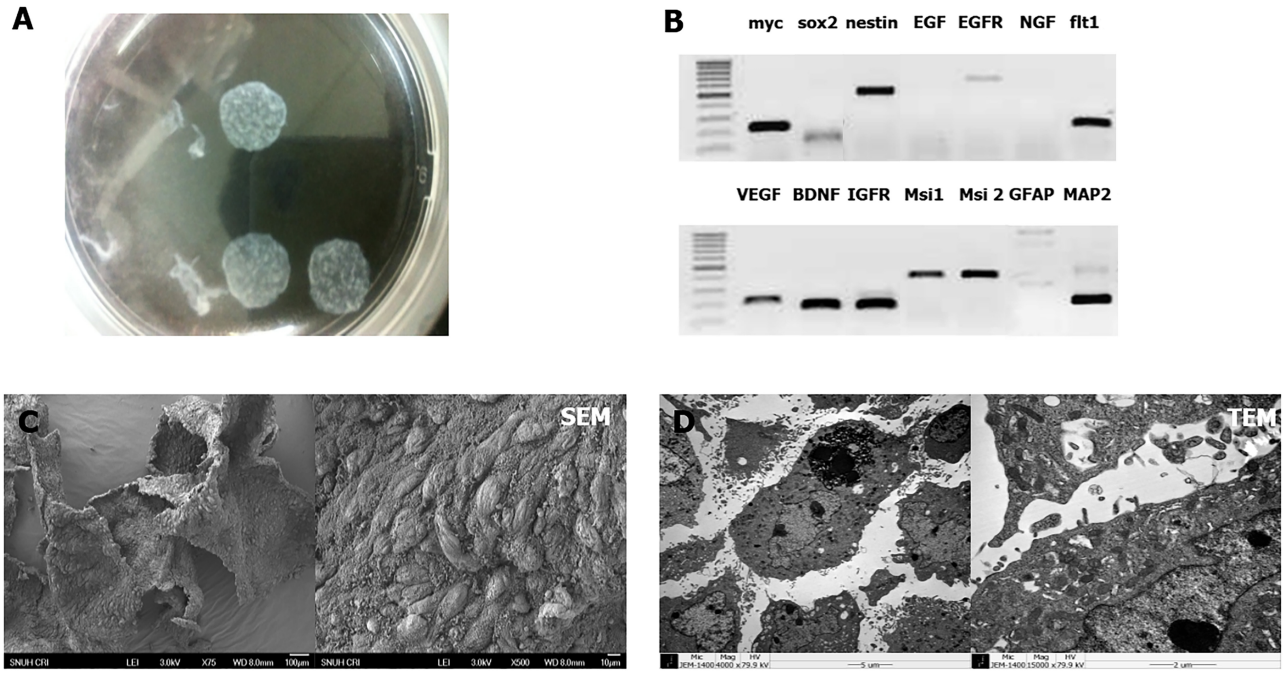

Figure 3. Cell sheet generation and characteristics. (A) Cell sheets are disc-like layers of human adipose tissue-derived stromal cells with olfactory neuroepithelial cells. (B) On reverse transcription polymerase chain reaction (RT-PCR) analysis (composite image), the cell sheet showed a high expression of stem cell markers including *myc*, *Msi1*, and *Msi2*; markers for neuronal development such as *sox2*, nestin, and *MAP2*; and various cytokines known to enhance and maintain cell proliferation and survival, such as *BDNF*[37] and *VEGF*[38]. (C) Scanning electron microscopy (SEM) evaluation of cell sheet surface reveals a sheet-like, organized, dense structure with high cellularity, composed of rich extracellular matrices and no necrotic core. (D) Transmission electron microscopy (TEM) demonstrates active intercellular molecule transfer. *Myc*, V-Myc avian myelocytomatosis viral oncogene homolog; *Sox2*, sex-determining region Y Box 2; *EGF*, epidermal growth factor; *EGFR*, EGF receptor; *NGF*, nerve growth factor; *flt1*, Fms-related tyrosine kinase 1 [or vascular endothelial growth factor receptor 1 (*VEGFR1*)]; *BDNF*, brain-derived neurotrophic factor; *IGFR*, insulin-like growth factor receptor 1; *Msi1*, Musashi RNA-binding protein 1; *GFAP*, glial fibrillary-associated protein; *MAP2*, microtubule-associated protein 2.

Ki-67, a proliferation marker, suggesting an active cell cycle state (Fig. 4H).

ICH Model Characteristics

Among the 24 animals with ICH induction, 7 (29.2%) animals died, all of which occurred within 48 h after the surgery. A postmortem MRI evaluation revealed a brain herniation associated with a sizeable hematoma and subsequent brain edema (Fig. 1F). After excluding the dead animals, 17 dogs were randomly assigned for transplantation analysis (9 in the control group and 8 in the cell sheet group) at 2 weeks after ICH. The mean hematoma volume in these 17 animals was 8.9±1.6 ml, and the median value was 9.1 ml (7.1–11.0 ml).

Cell Sheet Transplantation Reduced ICH-Related Hemispheric Atrophy

The MRI analysis for hemispheric atrophy showed that the atrophy of the hemispheres was significantly attenuated in the cell sheet group compared to the control group [control group: 12.4±4.6%, median=12.6% (8.3%–15.0%); cell sheet group: 8.1±3.3%, median=7.9% (5.3%–11.5%); $p=0.042$] (Fig. 5).

Cell Sheet Transplantation Did Not Enhance Functional Recovery After ICH

Both groups showed rapid and continuous functional improvement since the first week after ICH induction and exhibited near-complete improvement of the functional status on day 42. Consequently, no significant difference was observed in the results of the neurobehavioral tests over 6 weeks. However, the cell sheet group showed a tendency for a better functional status on day 35 compared to the control group, but the difference was not statistically significant ($p=0.062$) (Fig. 6).

Histological Examination

At 4 weeks after transplantation, the border of the cell sheet was invisible to the unaided eye but could be detected with GFP staining in the eight dogs that underwent transplantation. Most GFP^+ cells were clustered along the cortex overlying the hematoma (Fig. 7A and B),

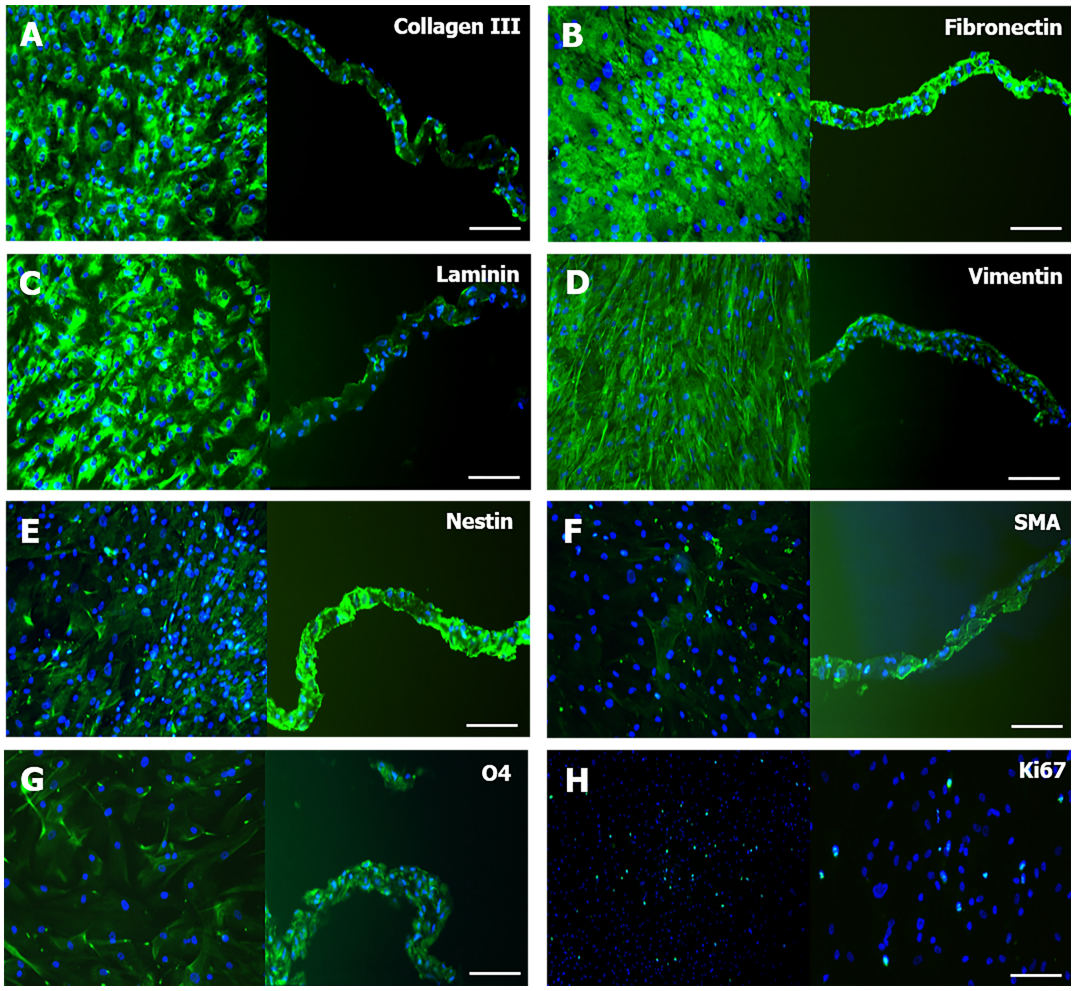

Figure 4. Immunocytochemistry of composite cell sheet. Cell sheet shows immunoreactivities (green) to (A) collagen III, (B) fibronectin, (C) laminin, (D) vimentin, (E) nestin, (F) smooth muscle actin (SMA), (G) oligodendrocyte 4 (O4), and (H) Ki-67. Left: transverse images; right: longitudinal images. Scale bars: 30 μm. Nuclei were counterstained with 4′,6-diamidino-2-phenylindole (DAPI).

and some migrated and were located in the perihematomal area (Fig. 7C). There was no significant gross or histological evidence of immune rejection around the cell sheet 4 weeks after transplantation. On immunostaining with antibodies for GFP, nestin, PDGFRβ, NF, and GFAP, the clustered cells showed positivity for both GFP and nestin, and the scattered GFP^+ cells were distributed around the hematoma, even into the lower margin of the hematoma (4.8 mm from the remnant sheet) (Fig. 7F). The scattered GFP^+ cells were located mainly in the perivascular space, expressing a pericyte marker PDGFRβ (30% of scattered GFP^+ cells) (Fig. 7I), or located in the adjacent parenchyma, expressing a neuronal marker NF (20% of scattered GFP^+ cells) (Fig. 7J). Astroglial differentiation of $GFAP^+$ transplanted cells was observed in only <1% of the scattered GFP^+ cells (Fig. 7O). A few GFP^+ cells were also noted in the contralateral hemisphere.

DISCUSSION

In this study, we generated a cell sheet composed of neural progenitor cells from the nasal neuroepithelium and adipose tissue stromal cells. The application of the cell sheet was feasible in a canine ICH model, the transplanted cells successfully survived for 4 weeks, and a considerable portion of the transplanted cells migrated to the perihematomal site and differentiated into neurons or pericytes. Furthermore, cell sheet transplantation alleviated ICH-related hemispheric atrophy and showed tendency for improving functional recovery.

It is clinically important that we performed cell sheet transplantation in the subacute stage of ICH. Previously, many trials to evaluate the benefit of stem cell delivery have been performed with various animal species, type and amount of stem cells, and route of administration in the experimental ICH[7,9,11]. In those studies, transplantation

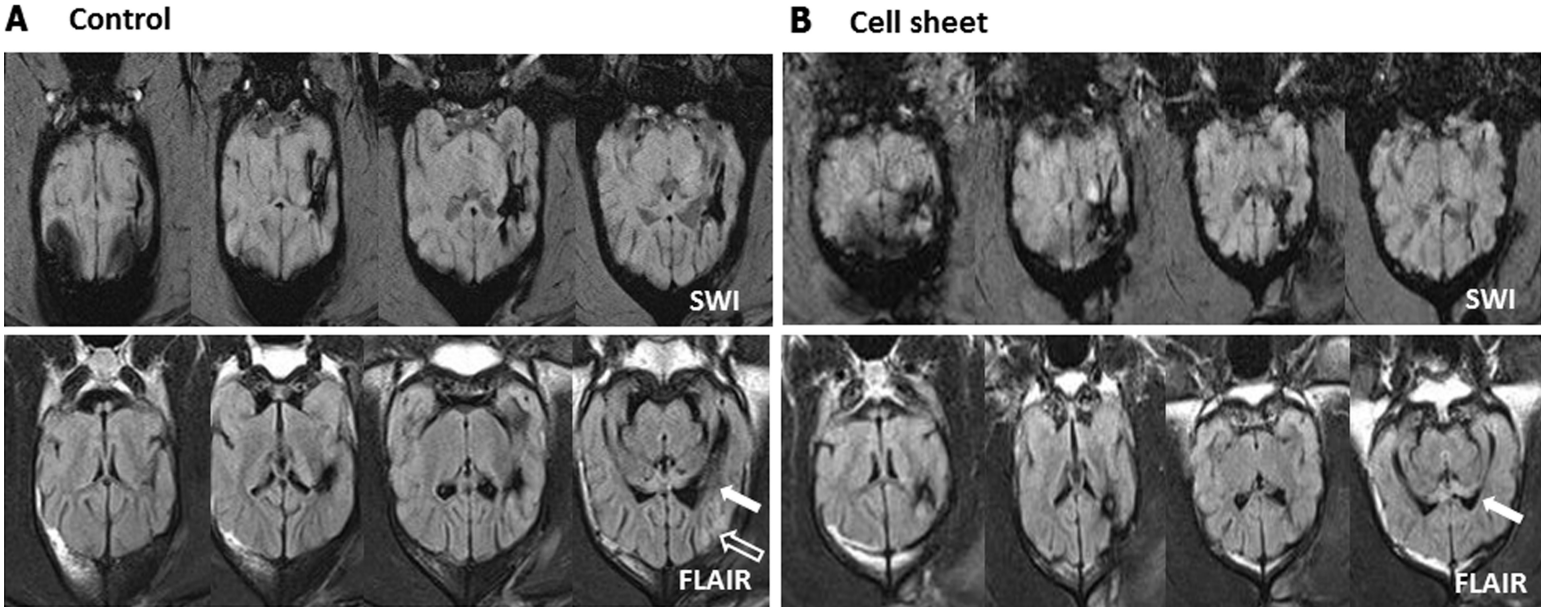

Figure 5. Brain atrophy evaluation by magnetic resonance imaging (MRI). Representative SWI and fluid-attenuated inversion recovery (FLAIR) images from the control group (A) and cell sheet group (B) at 6 weeks after ICH induction. In the FLAIR images, atrophic changes in the temporoparietal cortex (hollow arrow) associated with ventricle enlargement (white arrow) are observed in the control group. In the cell sheet group, only slight atrophic changes in the cortex are found with symmetric lateral ventricles (white arrow). In SWI images, chronic hematomas at temporoparietal cortexes are observed in both groups.

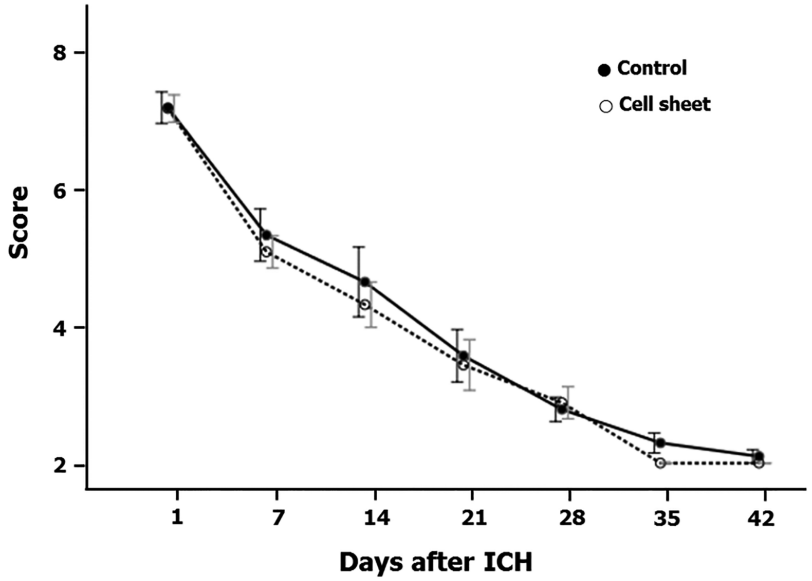

Figure 6. Neurobehavioral recovery curve. Six-week neurobehavioral tests reveal no significant difference between the control and cell sheet groups.

of cells was performed in acute stages (≤24 h) of ICH, and the reported efficacy of neural regeneration was low, ranging from 0% to 10%. Therefore, the bystander effect was suggested to be the main mechanism of functional benefit in stem cell treatment[7,9,11]. However, cell transplantation performed at the subacute stage in this study induced a significant migration of stem cells to the brain parenchyma and differentiation into neurons or pericytes. These findings might suggest that a direct cellular regeneration can be achieved in subacute disease stages by cell sheet transplantation of composite progenitor cells[7,8,11,13,14]. Accordingly, cell sheet transplantation might be a feasible dimension of neurosurgical intervention with great therapeutic potentials in treating ICH and other destructive CNS diseases. Furthermore, to the best of our knowledge, this is the first study to demonstrate the feasibility of cell sheet transplantation in a CNS disease model.

There are several possible mechanisms of enhanced cell survival and differentiation capacity after transplantation. The transplanted cell sheet possessed intact tissue integrity, which cannot be achieved by single-cell delivery techniques[12,16,22]. A sheet-like dense amalgamation of cells and the extracellular matrix on electron microscopy and a high expression of collagen III, fibronectin, and laminin on immunocytochemistry are essential for survival and engraftment of the transplanted cells. Another notable mechanism is that the adipose stromal cells within the sheet might have conferred the tissue microenvironment favorable for neural survival and proliferation. Adipose stem cells secrete cytokines that are associated with the functions of neuroprotection and cell proliferation and that modulate immune-mediated inflammatory reaction[7,14–16,18,20,22]. In the current study, the cell sheet showed a high expression of neuroprotective cytokines such as BDNF and VEGF and had a good capacity for self-proliferation. Additionally, adipose tissue might supply the cell pool for neovascularization[15,18,21]. A previous study regarding adipose tissue-derived cell sheet therapy for cardiac regeneration had demonstrated neovascularization from the cell sheet to the infarcted tissue soon after transplantation[15,18,21]. We also observed indirect evidence of beneficial effect of cell sheet for neovascularization, as a high expression of VEGF and FLT1 in the cell sheet. These multidirectional cell sheet activities might have achieved substantial cell survival and neurovascular regeneration.

Cell sheet transplantation has several clinical advantages over previously introduced cell delivery methods. Compared to conventional intravenous injection, which has a low efficacy of cell survival in the targeted tissue[7,11], cell composites within the sheet could survive easily at the cortex overlying the hematoma. Considering that the sheet cells surviving at the overlying cortex may further migrate to the perihematomal area and serve as a source of neurovascular regeneration, as well as exhibiting as the bystander effect, cell sheet transplantation might have a more potent benefit over intravenous injection. Furthermore, unlike the intracerebral injection of stem cells, cell sheet transplantation has a lower risk of intraparenchymal mass formation, leaves no scars along the injection route, and can be readily injected via a burr hole in the subacute period of ICH[2,11,17]. Therefore, cell

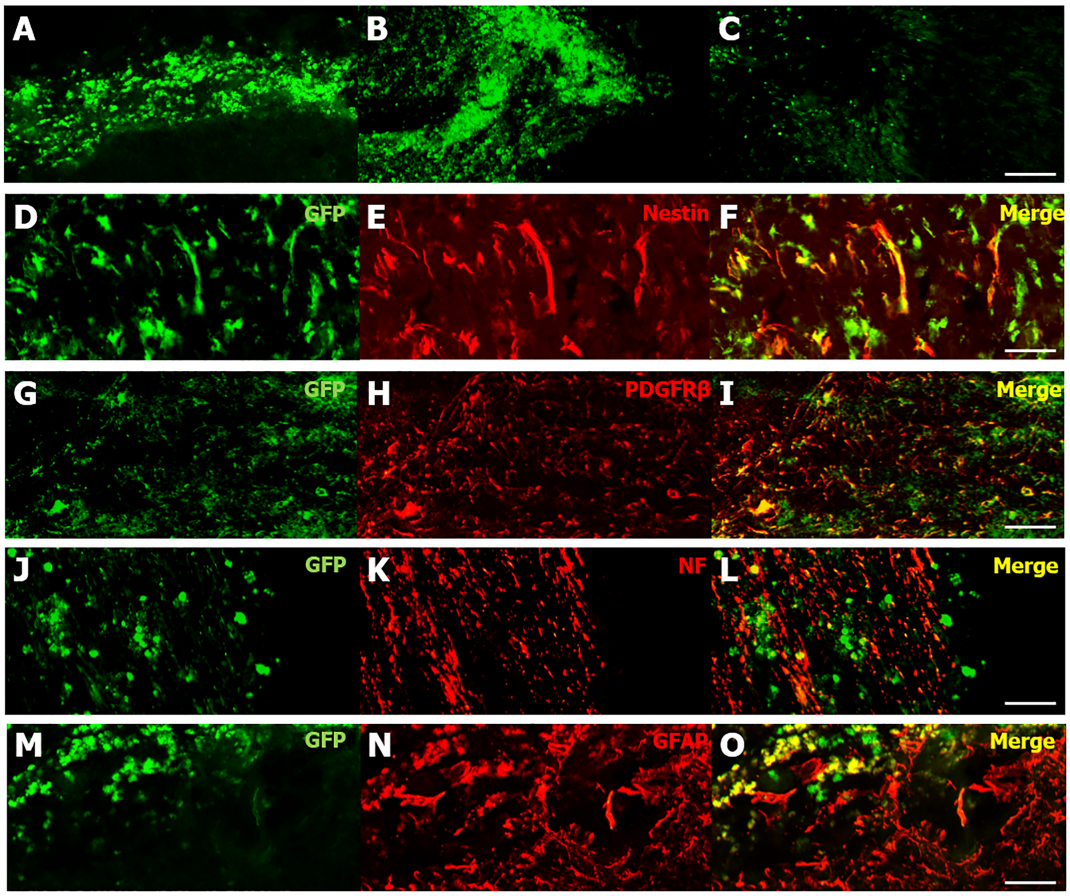

Figure 7. Engraftment and differentiation of transplanted cell sheet. The transplanted (GFP^+) cells were clustered in a layer-like appearance mainly in the cortex overlying the hemorrhagic lesion (A, B), and some cells were migrated and scattered around the lesion (C). When the brain sections were stained with antibodies for GFP, nestin (D–F), PDGFRβ (G–I), NF (J–L), and GFAP (M–O), the majority of GFP^+ cells were also positive for nestin (D–F). About 30% of the GFP^+ cells coexpressed PDGFRβ (G–I), mainly in the perivascular space (I, left side), and 20% of the GFP^+ cells in the parenchyma coexpressed a neuronal marker, NF (J–L), whereas they rarely expressed GFAP (M–O). Scale bars: 200 μm (A–C), 30 μm (D–O). GFP, green fluorescent protein; PDGFRβ, platelet-derived growth factor receptor β; NF, neurofilament.

sheet transplantation might be a more clinically applicable neurosurgical approach than the intracerebral injection method.

The major limitation to be addressed in this study is the negative result in the functional outcome analysis. We observed only an equivocal functional improvement on day 35 from ICH induction. This might be related with that every animal of ICH model in this study showed rapid improvement in neurological deficits immediately after the disease induction, without leaving significant neurologic sequelae. Therefore, the negative result might be due to the mild severity of disease in this experimental protocol. Infusion of a larger volume of hematoma was inapplicable owing to high mortality rates. Monitoring of intracranial pressure (ICP) and managing increased ICP (IICP) in the acute stage of ICH might be a good option to improve the clinical efficacy of the current model by minimizing IICP-related mortality even with larger volume of hematoma, consequently enabling a canine ICH model with more permanent neurologic damage. However, considering that the other outcome parameter, a degree of hemorrhage-associated hemispheric atrophy, had a statistically significant positive result, our study result might be interpreted to have some partially positive results regarding the effectiveness of cell sheet transplantation. Lack of quantitative analyses of the RT-PCR evaluation and comparative analyses of stem cell survival, migration, and differentiation between the cell sheet transplantation and single-cell suspension are also limitations of this study.

CONCLUSION

Our results show that neural progenitor cells can be effectively delivered as a cell sheet with adipose stromal

cells. After transplantation, cells from the cell sheet migrated to the perihematomal area and differentiated into neurons and pericytes, resulting in direct neural regeneration. The cell sheet transplantation was associated with modest functional improvement and effective prevention in hemispheric atrophy after ICH. Our strategy to use a scaffold-free cell sheet would be a useful neurosurgical intervention in improving the neurologic outcomes of ICH.

ACKNOWLEDGMENT: This study was supported by the Basic Science Research Program through the National Research Foundation of Korea (NRF), funded by the Ministry of Education, Science and Technology (Grant No. 2012R1A1A2002081). K.-H. Jung was supported by research grant from Ildong Pharmaceutical Co., Ltd. (0620110350), Chong Kun Dang Pharmaceutical Corp. (0620111230), and JW Pharmaceutical Co., Ltd. (0620132630). The authors declare no conflicts of interest.

REFERENCES

1. van Asch CJ, Luitse MJ, Rinkel GJ, van der Tweel I, Algra A, Klijn CJ. Incidence, case fatality, and functional outcome of intracerebral haemorrhage over time, according to age, sex, and ethnic origin: A systematic review and meta-analysis. Lancet Neurol. 2010;9(2):167–76.
2. Zhu J, Xiao Y, Li Z, Han F, Xiao T, Zhang Z, Geng F. Efficacy of surgery combined with autologous bone marrow stromal cell transplantation for treatment of intracerebral hemorrhage. Stem Cells Int. 2015;2015:318269.
3. Morgenstern L, Frankowski R, Shedden P, Pasteur W, Grotta J. Surgical treatment for intracerebral hemorrhage (STICH): A single-center, randomized clinical trial. Neurology 1998;51(5):1359–63.
4. Zuccarello M, Brott T, Derex L, Kothari R, Sauerbeck L, Tew J, Van Loveren H, Yeh H-S, Tomsick T, Pancioli A. Early surgical treatment for supratentorial intracerebral hemorrhage a randomized feasibility study. Stroke 1999; 30(9):1833–9.
5. NINDS ICH Workshop Participants. Priorities for clinical research in intracerebral hemorrhage: Report from a national institute of neurological disorders and stroke workshop. Stroke 2005;36(3):e23–41.
6. Qureshi AI, Wilson DA, Traystman RJ. Treatment of elevated intracranial pressure in experimental intracerebral hemorrhage: Comparison between mannitol and hypertonic saline. Neurosurgery 1999;44(5):1055–63.
7. Kim J-M, Lee S-T, Chu K, Jung K-H, Song E-C, Kim S-J, Sinn D-I, Kim J-H, Park D-K, Kang K-M. Systemic transplantation of human adipose stem cells attenuated cerebral inflammation and degeneration in a hemorrhagic stroke model. Brain Res. 2007;1183:43–50.
8. Ma X, Qin J, Song B, Shi C, Zhang R, Liu X, Ji Y, Ji W, Gong G, Xu Y. Stem cell-based therapies for intracerebral hemorrhage in animal model: A meta-analysis. Neurol Sci. 2015;36(8):1311–7.
9. Jeong S-W, Chu K, Jung K-H, Kim SU, Kim M, Roh J-K. Human neural stem cell transplantation promotes functional recovery in rats with experimental intracerebral hemorrhage. Stroke 2003;34(9):2258–63.
10. Wang C, Fei Y, Xu C, Zhao Y, Pan Y. Bone marrow mesenchymal stem cells ameliorate neurological deficits and blood-brain barrier dysfunction after intracerebral hemorrhage in spontaneously hypertensive rats. Int J Clin Exp Pathol. 2015;8(5):4715.
11. Lee S-T, Chu K, Jung K-H, Kim S-J, Kim D-H, Kang K-M, Hong NH, Kim J-H, Ban J-J, Park H-K. Anti-inflammatory mechanism of intravascular neural stem cell transplantation in haemorrhagic stroke. Brain 2008;131(3):616–29.
12. Kelm JM, Fussenegger M. Scaffold-free cell delivery for use in regenerative medicine. Adv Drug Deliv Rev. 2010; 62(7):753–64.
13. Zhang JJ. Mechanisms of cell therapy for clinical investigations: An urgent need for large-animal models. Circulation 2013;128(2):92–4.
14. Wilson A, Butler PE, Seifalian AM. Adipose-derived stem cells for clinical applications: A review. Cell Prolif. 2011;44(1):86–98.
15. Asakawa N, Shimizu T, Tsuda Y, Sekiya S, Sasagawa T, Yamato M, Fukai F, Okano T. Pre-vascularization of in vitro three-dimensional tissues created by cell sheet engineering. Biomaterials 2010;31(14):3903–9.
16. Labbé B, Marceau-Fortier G, Fradette J. Cell sheet technology for tissue engineering: The self-assembly approach using adipose-derived stromal cells. Methods Mol Biol. 2011;702:429–41.
17. Bible E, Chau DY, Alexander MR, Price J, Shakesheff KM, Modo M. Attachment of stem cells to scaffold particles for intra-cerebral transplantation. Nat Protoc. 2009; 4(10):1440–53.
18. Zakharova L, Mastroeni D, Mutlu N, Molina M, Goldman S, Diethrich E, Gaballa MA. Transplantation of cardiac progenitor cell sheet onto infarcted heart promotes cardiogenesis and improves function. Cardiovasc Res. 2010;87(1):40–9.
19. Miyagawa S, Saito A, Sakaguchi T, Yoshikawa Y, Yamauchi T, Imanishi Y, Kawaguchi N, Teramoto N, Matsuura N, Iida H. Impaired myocardium regeneration with skeletal cell sheets—A preclinical trial for tissue-engineered regeneration therapy. Transplantation 2010;90(4):364–72.
20. Hamdi H, Planat-Benard V, Bel A, Puymirat E, Geha R, Pidial L, Nematalla H, Bellamy V, Bouaziz P, Peyrard S. Epicardial adipose stem cell sheets results in greater post-infarction survival than intramyocardial injections. Cardiovasc Res. 2011;91(3):483–91.
21. Sekine H, Shimizu T, Hobo K, Sekiya S, Yang J, Yamato M, Kurosawa H, Kobayashi E, Okano T. Endothelial cell coculture within tissue-engineered cardiomyocyte sheets enhances neovascularization and improves cardiac function of ischemic hearts. Circulation 2008;118(14 suppl 1):S145–S52.
22. Bel A, Planat-Bernard V, Saito A, Bonnevie L, Bellamy V, Sabbah L, Bellabas L, Brinon B, Vanneaux V, Pradeau P. Composite cell sheets: A further step toward safe and effective myocardial regeneration by cardiac progenitors derived from embryonic stem cells. Circulation 2010;122 (11 Suppl 1):S118–S23.
23. Tsumanuma Y, Iwata T, Washio K, Yoshida T, Yamada A, Takagi R, Ohno T, Lin K, Yamato M, Ishikawa I. Comparison of different tissue-derived stem cell sheets for periodontal regeneration in a canine 1-wall defect model. Biomaterials 2011;32(25):5819–25.
24. Nakamura A, Akahane M, Shigematsu H, Tadokoro M, Morita Y, Ohgushi H, Dohi Y, Imamura T, Tanaka Y. Cell sheet transplantation of cultured mesenchymal stem cells enhances bone formation in a rat nonunion model. Bone 2010;46(2):418–24.

25. Yeh Y-C, Lee W-Y, Yu C-L, Hwang S-M, Chung M-F, Hsu L-W, Chang Y, Lin W-W, Tsai M-S, Wei H-J. Cardiac repair with injectable cell sheet fragments of human amniotic fluid stem cells in an immune-suppressed rat model. Biomaterials 2010;31(25):6444–53.
26. Fedak PW. Cardiac progenitor cell sheet regenerates myocardium and renews hope for translation. Cardiovasc Res. 2010;87(1):8–9.
27. Ding G, Liu Y, Wang W, Wei F, Liu D, Fan Z, An Y, Zhang C, Wang S. Allogeneic periodontal ligament stem cell therapy for periodontitis in swine. Stem Cells 2010;28(10):1829–38.
28. Granger N, Blamires H, Franklin RJ, Jeffery ND. Autologous olfactory mucosal cell transplants in clinical spinal cord injury: A randomized double-blinded trial in a canine translational model. Brain 2012;135(11):3227–37.
29. Féron F, Perry C, McGrath JJ, Mackay-Sim A. New techniques for biopsy and culture of human olfactory epithelial neurons. Arch Otolaryngol Head Neck Surg. 1998;124(8):861–6.
30. Lee RH, Kim B, Choi I, Kim H, Choi H, Suh K, Bae YC, Jung JS. Characterization and expression analysis of mesenchymal stem cells from human bone marrow and adipose tissue. Cell Physiol Biochem. 2004;14(4–6):311–24.
31. Jung KH, Chu K, Lee ST, Song EC, Sinn DI, Kim JM, Kim SJ, Kim JH, Kang KM, Park HK. Identification of neuronal outgrowth cells from peripheral blood of stroke patients. Ann Neurol. 2008;63(3):312–22.
32. Qureshi AI, Suri MFK, Ling GS, Khan J, Guterman LR, Hopkins LN. Absence of early proinflammatory cytokine expression in experimental intracerebral hemorrhage. Neurosurgery 2001;49(2):416–21.
33. Kidwell CS, Chalela JA, Saver JL, Starkman S, Hill MD, Demchuk AM, Butman JA, Patronas N, Alger JR, Latour LL. Comparison of MRI and CT for detection of acute intracerebral hemorrhage. JAMA 2004;292(15):1823–30.
34. Kothari RU, Brott T, Broderick JP, Barsan WG, Sauerbeck LR, Zuccarello M, Khoury J. The ABCs of measuring intracerebral hemorrhage volumes. Stroke 1996;27(8):1304–5.
35. Youn SW, Jung K-H, Chu K, Lee J-Y, Lee S-T, Bahn J, Park D-K, Yu J-S, Kim S-Y, Kim M. Feasibility and safety of intraarterial pericyte progenitor cell delivery following mannitol-induced transient blood? Brain barrier opening in a canine model. Cell Transplant. 2015;24(8):1469–79.
36. Chung DJ, Choi CB, Lee SH, Kang EH, Lee JH, Hwang SH, Han H, Lee JH, Choe BY, Lee SY. Intraarterially delivered human umbilical cord blood-derived mesenchymal stem cells in canine cerebral ischemia. J Neurosci Res. 2009;87(16):3554–67.
37. Hughes PE, Alexi T, Walton M, Williams CE, Dragunow M, Clark RG, Gluckman PD. Activity and injury-dependent expression of inducible transcription factors, growth factors and apoptosis-related genes within the central nervous system. Prog Neurobiol. 1999;57(4):421–50.
38. Rosenstein JM, Krum JM. New roles for VEGF in nervous tissue—Beyond blood vessels. Exp Neurol. 2004;187(2):246–53.